Formation of binary alloy cluster ions from group-14 elements and cobalt and comparison with solid-state alloys

6 AUTHORS, INCLUDING:

Xia Zhang
Shandong Cancer Hospital (Shandong Prov…
243 PUBLICATIONS **2,095** CITATIONS

SEE PROFILE

Guoliang Li
Universität Stuttgart
15 PUBLICATIONS **340** CITATIONS

SEE PROFILE

Zichao Tang
Chinese Academy of Sciences
66 PUBLICATIONS **517** CITATIONS

SEE PROFILE

Zhen Gao
Chinese Academy of Sciences
39 PUBLICATIONS **348** CITATIONS

SEE PROFILE

RCM

Formation of binary alloy cluster ions from group-14 elements and cobalt and comparison with solid-state alloys

Xia Zhang, Guoliang Li, Xiaopeng Xing, Xiang Zhao, Zichao Tang and Zhen Gao*

State Key Laboratory of Molecular Reaction Dynamics, The Center for Molecular Sciences, Institute of Chemistry, Chinese Academy of Sciences, Beijing 100080, China

By using laser ablation on mixtures of transition metal cobalt and group-14 elements, binary alloy cluster anions were produced while no binary alloy cluster cations were detected, and the homocluster cations of group-14 elements appeared at very low abundance. The differences between clustering abilities of germanium, tin and lead with cobalt are described, and the chemical bonds in the binary alloy cluster anions appear to indicate a transition from covalent to metal bonds. The cluster anion $[CoPb_{10}]^-$ appears in very high abundance (magic number), and an endohedral structure is proposed for this cluster. The cluster anion $[CoPb_{12}]^-$, also representing a magic number, probably has an icosahedral structure. Compared with solid-state Co/Ge binary alloys, the compositions of most binary alloy cluster anions are germanium-rich, in which the covalent bonds are predominant. Copyright © 2001 John Wiley & Sons, Ltd.

Alloy materials consisting of transition metal and group-14 elements have been widely investigated in materials science because the elements of group 14 can form alloys with many metal and non-metal elements. Transition metal silicides and germanides are potential materials for solid-state electronic devices. Binary T/Ge and ternary T/Ge/Si alloys (where T is a transition metal) are currently receiving much attention as promising candidates for low-resistivity interconnect lines and contacts to silicon substrates in Si-based semiconductor devices.[1] These binary and ternary germanides possess low room-temperature resistivity, high thermal stability and good adherence to silicon substrates. Tin alloys belong to the class of fusible alloys, and lead is a raw material for lead-based alloys. Because a small change in composition can lead to special properties, many systems such as T/Sn, Au/T/Sn and Sn/Pb[2–6] have also been studied.

In recent years, the investigations of these systems have focused on the stabilities of alloy compounds so as to obtain reliable thermodynamic data, exact phase diagrams, crystal compositions and crystal structures, as well as an understanding of factors affecting strengths of chemical bonds in these compounds.[3–13] However, the clustering behavior of group-14 elements with transition metals produced by laser ablation have not yet been reported to our knowledge. In order to broaden our understanding of thermodynamic stability and bonding trends in binary transition metal-metalloid (group-14 elements) alloy systems, a series of binary alloy cluster anions, produced by laser ablation of mixtures of Co/E (where E is Ge, Sn or Pb), were studied with a tandem time-of-flight (TOF) mass spectrometer. The stable compositions and the bonding trends in binary alloy cluster ions are also discussed in this paper. The properties of cluster anions $[Co_xGe_y]^-$, such as compositions and chemical bonding, are compared with those of Co/Ge binary alloys in the solid state.

EXPERIMENTAL

The binary alloy cluster ions of group-14 elements (E) and the transition metal cobalt were generated and analyzed under the following conditions. The samples were prepared with E (germanium purity: 99.99%, tin purity: 99.9%, lead purity: 99.8%) and cobalt (purity 99.9%) powders, mixed well in different atomic ratios and pressed into tablets.

The experiments to produce and detect Co/E binary cluster ions were performed using a vaporization laser together with the first stage of a home-made tandem time-of-flight mass spectrometer (T-TOF-MS). A detailed description of the T-TOF-MS has been given elsewhere.[14] Briefly, the second harmonic of a Q-switched Nd:YAG laser (532 nm, 10 mJ/pulse, 10 pulse/s) was focused on the surface of a tablet sample held in the vacuum chamber (at 10^{-6} Torr) of the spectrometer to produce the cluster ions. The cluster ions were extracted and accelerated with a pulse voltage of 0.1 V and 1.1 kV, respectively, and then drifted in a field-free region 3.5 m long. The cluster ions were detected by a dual microchannel plate detector at the end of the field-free region, and recorded to give the mass spectrum. The mass resolution of the first stage of the T-TOF-MS is about 300.

Correspondence to: Z. Gao, State Key Laboratory of Molecular Reaction Dynamics, The Center for Molecular Sciences, Institute of Chemistry, Chinese Academy of Sciences, Beijing 100080, China.
E-mail: gaoz@mrdlab.icas.ac.cn

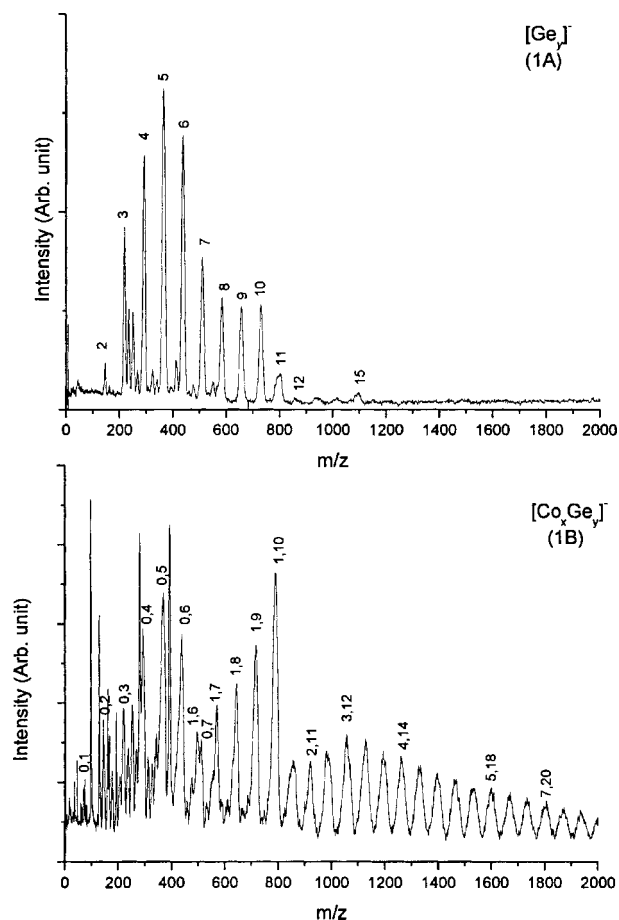**Figure 1.** TOF mass spectra of $[Ge_y]^-$ and $[Co_xGe_y]^-$ produced by laser ablation of pure Ge and mixed samples of Co and Ge: (A) elemental Ge; (B) Ge/Co = 1:2.

Figure 2. TOF mass spectra of $[Sn_y]^-$ and $[Co_xSn_y]^-$ produced by laser ablation of pure Sn and mixed samples of Co and Sn: (A) elemental Sn; (B) Sn/Co = 1:2.

Typically, 1000–2000 laser shots were accumulated and stored in a PC computer.

RESULTS

Figures 1(A) and 1(B) show the mass spectrum of anions resulting from the pure germanium sample and the cluster anion distribution resulting from the sample with atomic ratio Ge/Co = 1:2, respectively. It is clear, by comparing these two figures, that the resulting cluster distribution is mainly dominated by pure germanium clusters $[Ge_y]^-$ in the lower mass region (*m/z* between 0 and 450), and by Co/Ge binary alloy cluster anions in the higher mass region (*m/z* > 450). The binary alloy cluster anions $[CoGe_y]^-$ show a magic number at y = 10, with a very deep abundance minimum at y = 11. In our previous work[15] a cage structure of $[CoGe_{10}]^-$ was predicted. Furthermore, the binary cluster anions $[Co_xGe_y]^-$ (x > 1; y > 9) with more than one cobalt atom were also detected in the higher mass region, but their peaks are less intense than those of $[CoGe_y]^-$ (y = 6–11). In binary cluster anions $[Co_xGe_y]^-$ (x > 1; y > 9), the number of germanium atoms is much larger than that of cobalt atoms.

A typical spectrum of tin cluster anions produced by laser ablation of an elemental tin sample is shown in Fig. 2(A). The largest detected ion is a 15-atom cluster. Figure 2(B) resulted
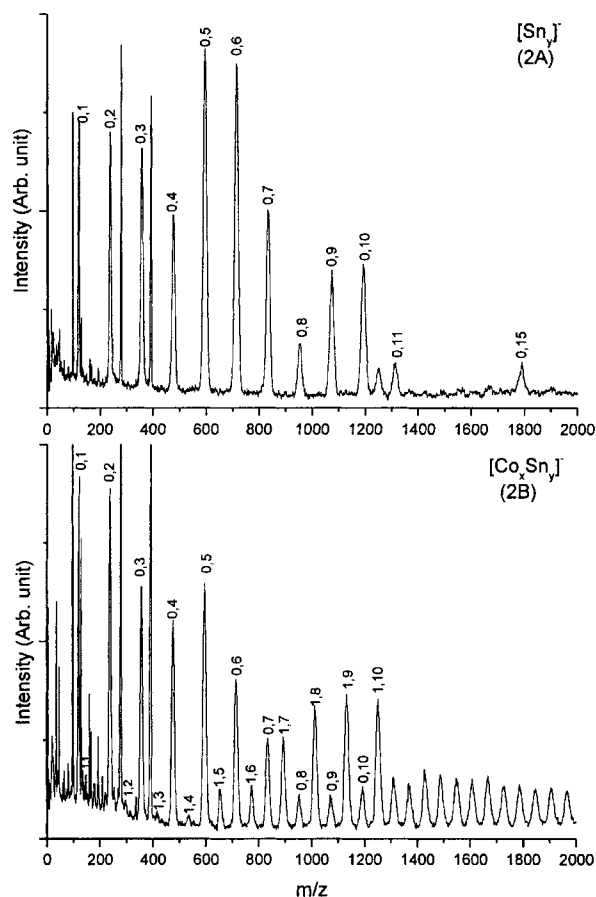
from the sample with atomic ratio Sn/Co = 1:2; $[Co_xSn_y]^-$ (x > 1; y > 10) and $CoSn_y^-$ are all generated. In contrast to the binary alloy cluster anions $[CoGe_y]^-$, the $[CoSn_y]^-$ binary alloy anionic clusters with minimum size y = 1 are observed. The homoatomic clusters $[Sn_y]^-$ are found with increased intensity in the lower mass region, again different from $[CoSn_y]^-$ clusters. When the number of tin atoms is 7, the $[CoSn_7]^-$ binary anionic cluster has an abundance similar to that of $[Sn_7]^-$. In the higher mass region, the peaks due to binary alloy cluster anions $[CoGe_y]^-$ (y > 7) are predominant, and the $[CoSn_y]^-$ (y = 8, 9, 10) clusters have similar abundances.

The mass spectrum of pure $[Pb_y]^-$ cluster anions is presented in Fig. 3(A). The size distributions for $[Pb_y]^-$ and $[Ge_y]^-$ anions are very similar, and the largest species detected is a 12-atom anionic cluster $[Pb_{12}]^-$. The mass spectrum in Fig. 3(B) shows that Co/Pb binary alloy cluster anions are obviously distinct from Co/Ge and Co/Sn binary alloy anionic clusters. In the mass region detected, three kinds of cluster anions were observed, namely, homocluster anions $[Pb_y]^-$, binary alloy cluster anions $[CoPb_y]^-$ (y = 1–12), and $[Co_2Pb_y]^-$ (y = 1–10). The relative abundances of $[Co_2Pb_y]^-$ (y = 1–10) anions are the lowest. When the number of lead atoms y ≤ 7, the $[Pb_y]^-$ clusters still dominate the other two kinds of binary clusters. However, for larger y (y > 7), $[CoPb_y]^-$ anions show higher abundances than $[Pb_y]^-$

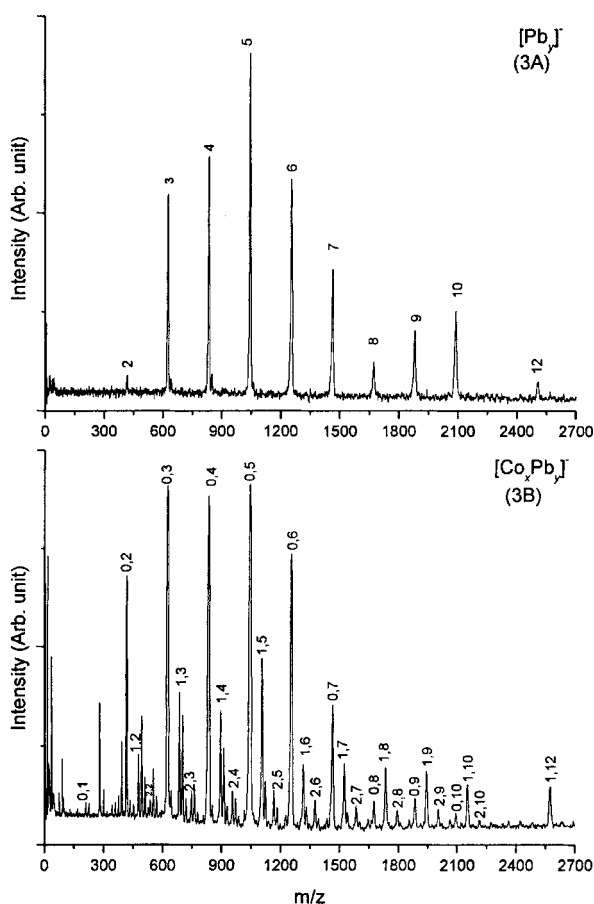**Figure 3.** TOF mass spectra of $[Pb_y]^-$ and $[Co_xPb_y]^-$ produced by laser ablation of pure Pb and mixed samples of Co and Pb: (A) elemental Pb; (B) Pb/Co = 1:2.

anions. In addition, several oxide-containing ternary cluster anions are observed: $[CoPb_yO]^-$, $[CoPb_yO_2]^-$, $[Co_2Pb_yO]^-$, $[Co_2Pb_yO_2]^-$ (y = 1–9), that probably arise from oxygen impurities on the surface of the samples during sample transfer to the mass spectrometer. It can be inferred that the ability to form Co/Pb/O ternary cluster anions is also strong.

In the laser ablation experiments on mixtures of cobalt and group-14 elements, binary alloy cluster cations were barely observable, and also the peaks of pure $[E_y]^+$ cluster cations even decreased or disappeared.

DISCUSSION

In our experiments, larger metal cluster ions hardly formed due to the poor cooling effect without carrier gas. However, the experiments show that the transition metal cobalt can easily cluster with group-14 elements to form binary alloy cluster anions, indicating that the ability of clustering between E and Co is strong, i.e. there are strong bonding interactions between Co and E.

In the case of homoclusters of E atoms formed by laser ablation, clusters $[E_y]^+$ with maximum size of y = 12, 10 and 10 are found for E = Ge, Sn, Pb, respectively, while $[E_y]^-$ anion species with maximum size up to y = 15 are observed ($[Ge_{15}]^-$, $[Sn_{15}]^-$, $[Pb_{12}]^-$). For laser ablation of the mixtures

of group-14 elements and cobalt, binary alloy cluster anions of larger size are observed, but no binary alloy cluster cations. This fact shows that the numbers of valence electrons in the binary alloy clusters, i.e. their electronic structures, are the key to the stability of the binary alloy clusters.

In the higher mass region, germanium, tin and cobalt can form larger binary alloy cluster anions that contain more than two cobalt atoms. However, there is a trend in that the number of cobalt atoms in binary alloy cluster anions is less than that of germanium or tin atoms. For example, the lead plus cobalt binary cluster anions contain only one or two cobalt atoms. Although the three group-14 elements can all form anions with Co in the lower mass region, the minimum sizes and the relative abundances of $[CoE_y]^-$ are very different. The number of E atoms in $[CoE_y]^-$ is y = 6–11 for Ge, and y = 1–10 for Pb and Sn. The relative abundances of the cluster anions $[CoGe_y]^-$ steadily increase as the number of Ge atoms increases from y = 6–10, with a sudden minimum in abundance for the cluster anion with y = 11 (Fig. 1(B)). The $[CoGe_{10}]^-$ cluster anion is considered to correspond to a magic number, and its reasonably predicted endohedral structure is a bicapped tetragonal antiprism.[15] In the cases of $[CoSn_y]^-$ and $[CoPb_y]^-$, a similar pattern of abundances of the binary cluster anions was not found, indicating that Ge, Sn and Pb have different bonding characteristics with Co.

It is known that the group-14 elements Ge, Sn and Pb can be self-bonding, but the ability of self-bonding decreases in the order Ge, Sn and Pb.[16] During the formation of binary alloy cluster anions $[Co_xE_y]^-$, two kinds of clustering process occur in the plasma, namely, homoclustering (group-14 element self-bonding) and heteroclustering (the bonding between a group-14 element and Co). Due to the decrease of self-bonding ability in the order Ge, Sn, Pb, the heteroclustering ability between cobalt and E elements increases from Ge to Pb. The analysis proposed above can explain the experimental observations that, in the lower mass region, cobalt atoms hardly cluster with germanium atoms and no binary cluster anions were generated, but cluster series $[CoSn_y]^-$ (y = 1–10) and $[Co_xPb_y]^-$ (x = 1–2; y = 1–12) were formed. The atomic radius of group-14 elements increases in the order Ge, Sn, Pb (Ge: 122.5 pm, Sn: 140.5 pm, Pb: 175.0 pm[17]). It is obvious that the Co atomic radius (125.3 pm[17]) is similar to that of germanium but is very different from that of lead. Therefore, in the clustering process, a cobalt atom might act as a gap-filling atom and insert into a cluster of lead atoms to participate in bonding with Pb. Smaller HOMO-LUMO gaps for clusters of the heavier elements E[18] also account for the fact that cobalt atoms easily bond with lead atoms. It has been reported that the transition from covalent to normal metal cluster growth in the group-14 elements occurs between tin and lead.[19] During the formation of binary alloy cluster anions $[Co_xE_y]^-$, this kind of transition may still exist, so that some differences are observed between Co/Sn and Co/Pb binary alloy cluster anions.

In Fig. 3(B), $[CoPb_y]^-$ cluster anions show relatively intense peaks at y = 5, 10, and 12, the magic numbers. The abundance profiles of $[Pb_y]^+$ clusters obtained by oven
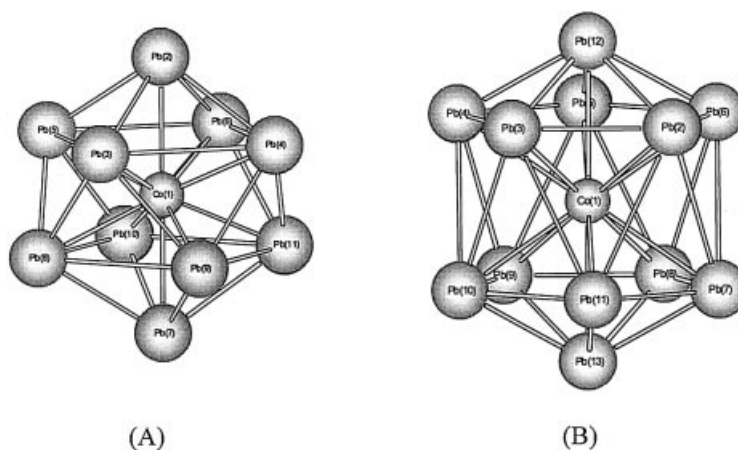
Figure 4. Possible structures of the $[CoPb_{10}]^-$ and $[CoPb_{12}]^-$ cluster anions. (A) bi-capped tetragonal antiprism structure of $[CoPb_{10}]^-$; (B) icosahedral structure of $[CoPb_{12}]^-$.

evaporation and ionization by 35 eV electrons[20] show magic numbers at y = 7, 10, 13, 17, and 19, with a very deep minimum at y = 14 which is probably due to single-atom evaporation[21] to yield the y = 13 cluster. The features at y = 13, 14 and 19 are similar to those seen[21] with $[Xe_y]^+$. It is known that crystalline Pb is closely packed, like the inert gases, and the interatomic interactions can be described in terms of soft-sphere atoms. The result is a pentagonal layer packing sequence 1,5,1,5,···1, that produces magic numbers at y = 7, 13 (icosahedron), 19 (bi-icosahedron), and so on.[22] Removal by evaporation of the tip atoms from y = 19 gives y = 17, and y = 10 is probably a 1,4,4,1 bi-capped square antiprism.[23] Therefore, we suggest that the $[CoPb_{10}]^-$ binary cluster anion may be a 1,4,<u>1</u>,4,1 bi-capped square antiprism (<u>1</u> represents a cobalt atom, the numbers without an underline represent lead atoms; Fig. 4(A)). The $[CoPb_{12}]^-$ binary cluster anion probably has an icosahedral structure with a small cobalt atom in the center of the cage, which is a pentagonal layer packing sequence 1,5,<u>1</u>,5,1 (Fig. 4(B)). Because a cobalt atom has seven 3d electrons, it can easily coordinate with lead atoms around it and make this icosahedral structure stable. This approach can explain why no Pb_{13}^- was observed, but the $[CoPb_{12}]^-$ binary cluster anion represents a magic number.

Comparison with solid-state phase alloys

A number of transition metal germanides, represented by formulas such as T_3Ge, T_2Ge, T_5Ge_3, $T_{11}Ge_8$, TGe, TGe_2 and TGe_{2-x} (T = transition metal), are known to exist in the binary transition metal-germanium systems.[24] Generally, in the binary equilibrium phase diagram, most germanium-rich phases are digermanides (TGe_2) or defect-digermanides (TGe_{2-x}).[25] Exceptions are the Mn-Ge and Ni-Ge systems, in which no intermetallic phases containing more than 50 at.-% Ge exist in the phase diagram. However, in the gas phase, the corresponding Co/Ge binary alloy cluster ions are not detected by the T-TOF-MS. Co/Ge binary alloy cluster anions mostly rich in germanium are easily produced. It can be inferred that the clustering behavior in the gas-phase anions is completely distinct from that for bulk solid-state

phase alloys. This difference is related to the mode of bonding between germanium and cobalt. The Pauling electronegativities (the values are 1.8 for both germanium and cobalt[26]) reveal that their abilities to bind electrons are equivalent. Therefore, in solid-state Co/Ge alloys, metal bonds between Co and Ge atoms provide the fundamental way of bonding. However, in the gas phase, the electron affinity is an important factor in the formation of cluster anions. The electron affinity of a germanium atom (1.233 eV)[27] is larger than that of a cobalt atom (0.662 eV),[28] so in the gas phase germanium atoms easily cluster with one another due to self-bonding. The experiments reveal that intense peaks due to pure $[Ge_y]^-$ are still observed even though the atomic ratio of Co to Ge is 8:1. The covalent bonds between germanium atoms are predominant, the primary mode of bonding is covalent, and the compositions are germanium-rich binary alloy anionic clusters.

CONCLUSIONS

Abundant binary alloy cluster anions were produced by laser ablation of mixtures of the transition metal cobalt plus group-14 elements (E). The heteroclustering ability between cobalt and E elements increases from Ge to Pb, and the chemical bonds in the corresponding binary alloy cluster anions might indicate a transition from covalent to metal bonds. An endohedral structure was predicted for the cluster anion $[CoPb_{10}]^-$ (magic number). The cluster anion $[CoPb_{12}]^-$ probably has an icosahedral structure, in which cobalt provides valence electrons and coordinates with the lead atoms around it. Compared with solid-phase Co/Ge binary alloys, the compositions of most binary alloy cluster anions are germanium-rich, in which covalent bonds are predominant.

REFERENCES

1. Silicides, germanides and their interfaces, In Fatheuer RW et al. (eds). *Materials Research Society Proceedings, vol. 320, MRS, 1993*, Part V.
2. Kjekshus A, Pearson WB. *Prog. Solid State Chem.* 1964; **1**: 83.
3. Neumann A, Kjekshus A, Romming C, Rost E. *J. Solid State Chem.* 1995; **119**: 142.
4. Neumann A, Kjekshus A, Romming C, Rost E. *J. Alloys Comp.* 1996; **240**: 42.
5. Neumann A, Bros H, Castanet R, Kjekshus A. *J. Alloys Comp.* 2000; **307**: 167.
6. Khairulin RA, Stankus SV, Bezverkhy PP. *J. Alloys Comp.* 2000; **312**: 211.
7. Takizawa H, Uheda K, Endo T. *J. Alloys Comp.* 2000; **305**: 306.
8. Zarembo S, Kematick RJ, Myers CE. *J. Alloys Comp.* 2000; **299**: 126.
9. Chastel R, Lbibb R, Castanet R. *J. Alloys Comp.* 1999; **283**: 208.
10. Sologub OL, Salamakha PS, Godart C. *J. Alloys Comp.* 2000; **307**: 31.
11. Khairulin RA, Stankus SV, Bezverkhy PP. *J. Alloys Comp.* 2000; **312**: 211.
12. Schmitt D, Ouladdiaf B, Routsi CD, Yakinthos JK, Gamari-Seale H. *J. Alloys Comp.* 1999; **292**: 21.
13. Zeng LM, Franzen HF. *J. Alloys Comp.* 2000; **313**: 75.
14. Yu ZD, Zhang N, Wu XJ, Gao Z, Zhu QH, Kong F. *J. Chem. Phys.* 1993; **99**: 1765.
15. Zhang X, Li GL, Gao Z. *Rapid Commun. Mass Spectrom.* 2001; **15**: 1573.
16. Zhang QL et al. Series of Inorganic Chemistry, vol. 3. Scientific Publishing Company, 1988; 324.
17. Zhou GD, Duan LY. *Base of Structural Chemistry* (2nd edn). Publishing Company of Peking University, 1995; 398.
18. Eber B, Buchholz D, Huttner G, Fassler TF, Imhof W, Fritz M, Daran JC, Jeannin YJ *Organomet. Chem.* 1991; **401**: 49.
19. Shvartsburg AA, Jarrold MF. *Chem. Phys. Lett.* 2000; **317**: 615.
20. Muhlbach J, Pfau P, Sattler K, Recknagel E. *Z. Phys. B.* 1982; **47**: 233.
21. Phillips JC. *Chem. Rev.* 1986; **86**: 619.
22. Hoare MR, Pal P. *Adv. Phys.* 1971; **20**: 161.
23. Phillips JC. *J Chem. Phys.* 1987; **87**: 1712.
24. Villars P, Calvert LD. *Pearson's Handbook of Crystallographic Data For Intermetallic Phases*, vols. 1–4. ASM International: Ohio, 1991.
25. Massalski TB, Okamoto H, Subramanian PR, Kacprzzak L (eds). *Binary Alloy Phase Diagrams* (2nd edn), vols. **1–3**, ASM International: Ohio, 1990.
26. Greenwood NN, Earnshaw A. *Chemistry of the Elements*, Pergamon Press: Oxford, New York.
27. Miller TM, Miller AES, Lineberger WC. *Phys. Rev. A* 1986; **33**: 3558.
28. Leopold DG, Lineberger WC. *J. Chem. Phys.* 1986; **85**: 51.